Enhanced regeneration of degraded polymer solar cells by thermal annealing

Pankaj Kumar, Chhinder Bilen, Krishna Feron, Xiaojing Zhou, Warwick J. Belcher, and Paul C. Dastoor

Citation: Applied Physics Letters **104**, 193905 (2014); doi: 10.1063/1.4878408
View online: http://dx.doi.org/10.1063/1.4878408
View Table of Contents: http://scitation.aip.org/content/aip/journal/apl/104/19?ver=pdfcov
Published by the AIP Publishing

Enhanced regeneration of degraded polymer solar cells by thermal annealing

Pankaj Kumar,[1,2,a)] Chhinder Bilen,[2] Krishna Feron,[2,3] Xiaojing Zhou,[2] Warwick J. Belcher,[2] and Paul C. Dastoor[2,b)]
[1]*CSIR-National Physical Laboratory, Dr. K. S. Krishnan Marg, New Delhi 110012, India*
[2]*Centre for Organic Electronics, Physics, University of Newcastle, Callaghan NSW-2308, Australia*
[3]*CSIRO Energy Technology, P. O. Box 330, Newcastle NSW 2300, Australia*

(Received 23 March 2014; accepted 6 May 2014; published online 14 May 2014)

The degradation and thermal regeneration of poly(3-hexylethiophene) (P3HT):[6,6]-phenyl-C_{61}-butyric acid methyl ester (PCBM) and P3HT:indene-C_{60} bisadduct (ICBA) polymer solar cells, with Ca/Al and Ca/Ag cathodes and indium tin oxide/poly(ethylene-dioxythiophene):polystyrene sulfonate anode have been investigated. Degradation occurs via a combination of three primary pathways: (1) cathodic oxidation, (2) active layer phase segregation, and (3) anodic diffusion. Fully degraded devices were subjected to thermal annealing under inert atmosphere. Degraded solar cells possessing Ca/Ag electrodes were observed to regenerate their performance, whereas solar cells having Ca/Al electrodes exhibited no significant regeneration of device characteristics after thermal annealing. Moreover, the solar cells with a P3HT:ICBA active layer exhibited enhanced regeneration compared to P3HT:PCBM active layer devices as a result of reduced changes to the active layer morphology. Devices combining a Ca/Ag cathode and P3HT:ICBA active layer demonstrated ~50% performance restoration over several degradation/regeneration cycles. © *2014 AIP Publishing LLC*. [http://dx.doi.org/10.1063/1.4878408]

Polymer solar cells (PSCs) have attracted increasing worldwide interest due to their unique material properties that allow the cost effective fabrication of thin, light weight, and mechanically flexible solar modules via high-throughput roll to roll production techniques.[1] In spite of many challenges, the power conversion efficiency of these devices has improved tremendously in the last decade, with *p*-type conjugated polymers blended with *n*-type fullerenes forming bulk heterojunction (BHJ) nanostructures showing the most efficient power conversion efficiencies. Single BHJ structures have demonstrated efficiencies of up to ~9%, whereas for tandem BHJ structures this value now exceeds the 10% watershed.[2–6] Moreover, there is still plenty of room for further improvement in the efficiency of these devices with 15%–20% efficient devices already predicted.[7]

In addition to improved power conversion efficiency, however, PSCs also need to be sufficiently stable in order to be commercially viable.[8,9] Thus, degradation is an equally important issue and typically the most efficient solar cells have yet to demonstrate high stability. Degradation of PSCs is a complicated process and involves the interplay of several degradation mechanisms.[1,8,10] Indeed, degradation occurs throughout the device structure, from top to bottom electrode, and causes a loss in the electronic and optical properties of the devices. Currently, much effort is underway by a number of research groups in order to understand the relevant degradation mechanisms and hence develop appropriate mitigation strategies.[8,11,12] It is well accepted that H_2O and O_2 molecules are the key moieties responsible for PSC degradation.[8,13,14] H_2O and O_2 molecules diffuse into the devices from the ambient surroundings and react with the different components in the device structure. For example, the hygroscopic poly(ethylene-dioxythiophene):polystyrene sulfonate (PEDOT:PSS) buffer layers used in PSCs readily absorb H_2O molecules from ambient and this process has been shown to cause rapid PSC degradation.[15] Protection of PSCs via encapsulation is the main approach currently being developed to impart good device stability, but fabricating low cost encapsulation materials with low H_2O and O_2 permeation rates remains a key challenge.[16,17] Replacement of the PEDOT:PSS buffer layer with less hygroscopic materials and the development of inverted solar cell structures have shown comparatively better stability even without encapsulation.[18,19] However, even after proper encapsulation these devices will still degrade through subsequent photo-chemical reactions, electrode diffusion, and morphological changes.[1] In this Letter, we present an alternative approach to increase the working lifespan of PSCs through the thermal regeneration of degraded devices. We have investigated the regeneration of PSCs based on blend films of poly (3-hexylethiophene) (P3HT):indene-C_{60} bisadduct (ICBA) and P3HT:[6,6]-phenyl-C_{61}-butyric acid methyl ester (PCBM), with Ca/Al and Ca/Ag cathodes by subjecting them to thermal annealing under inert atmosphere. We demonstrate that it is possible to regenerate PSCs even after several degradation/regeneration cycles and that the ability of a given PSC structure to regenerate depends both on the blend and cathode materials.

PSCs were prepared on cleaned indium tin oxide (ITO) coated glass substrates. A thin layer of PEDOT:PSS was coated onto the ITO substrates by spin coating at 4000 rpm for 90 s and dried at 140 °C for 30 min. Photoactive layers of both P3HT:ICBA and P3HT:PCBM blends (1:0.8) were spin coated from chloroform solutions (18 mg/ml) onto the PEDOT:PSS films in an inert atmosphere glove box at 2000 rpm for 60 s and pre-heated at 60 °C for 5 min.

[a)]Author to whom correspondence should be addressed. Electronic mail: pankaj@mail.nplindia.ernet.in
[b)]Email: Paul.Dastoor@newcastle.edu.au

Pre-heating of the active layers is done to remove the solvent traces in the active layer and 60 °C was found to be the optimum temperature for devices spun from chloroform. The substrates were transferred to a vacuum evaporation chamber where the Ca (20 nm) and Al (130 nm) or Ag (130 nm) cathode materials were deposited via thermal evaporation at $\sim 2 \times 10^{-6}$ millibars. After the cathode evaporation, the devices were subjected to thermal annealing in the glove box, where P3HT:PCBM devices were annealed at 140 °C for 5 min, and those based on P3HT:ICBA active layer were annealed at 160 °C for 5 min. The annealing times and temperatures were optimized for maximum power conversion efficiency. After preparation, the devices were stored in dark under ambient conditions and tested using a Newport AM 1.5G solar simulator. The solar cells were unencapsulated and the degradation studies were performed under ambient conditions (21 ± 2 °C and $55\% \pm 3\%$ relative humidity (RH)). Once the devices were dead the regeneration of device characteristics was achieved by subjecting the degraded devices to thermal annealing in a nitrogen inert atmosphere glove box. For regeneration, the fully degraded P3HT:PCBM devices were subjected to thermal annealing at 140 °C for 5 min, whereas those based on P3HT:ICBA active layer were subjected to thermal annealing at 160 °C for 5 min. A schematic design of the PSC structure is shown in Fig. 1(a). Fig. 1(b) shows the initial dark (solid symbols) and illuminated (open symbols) *J-V* characteristics for the P3HT:ICBA and P3HT:PCBM solar cells with Ca/Al and Ca/Ag cathodes. The short circuit current density (J_{sc}), open circuit voltage (V_{oc}), fill factor (*FF*), and the power conversion efficiency (η) of the PSCs are tabulated in Table I, where the error values corresponds to the standard deviation of measurements on six devices. The increased initial efficiency of the P3HT:ICBA devices compared to those based on PCBM arises from the higher V_{oc} of the ICBA solar cells, which can be attributed to the difference in lowest unoccupied molecular orbital (LUMO) level of the two acceptors.[20]

TABLE I. Photovoltaic parameters of PSCs with different active layers and different cathodes. The values in the bracket show the error calculated over the sets of 6 devices.

Active layer	Cathode	J_{sc} (mA/cm^2)	V_{oc} (V)	*FF* (%)	η (%)
P3HT:PCBM	Ca/Al	9.96 (0.40)	0.59 (0.00)	0.58 (0.01)	3.44 (0.45)
P3HT:PCBM	Ca/Ag	9.33 (0.50)	0.58 (0.01)	0.57 (0.04)	3.08 (0.30)
P3HT:ICBA	Ca/Al	9.60 (0.90)	0.83 (0.01)	0.52 (0.01)	4.30 (0.40)
P3HT:ICBA	Ca/Ag	9.90 (0.40)	0.81 (0.01)	0.51 (0.3)	4.25 (0.50)

Fig. 2(a) shows the degradation characteristics of η and V_{oc} for P3HT:ICBA solar cells with Ca/Ag cathodes. The solar cells were subjected to thermal annealing in the glove box when they were almost fully degraded and this process was repeated for subsequent degradation of the devices. Fig. 2(a) shows that the efficiency of the P3HT:ICBA solar cells exhibited a recovery of up to ~50% of the initial value, while the V_{oc} exhibited a recovery up to ~90% of the initial value. In addition the J_{sc} and *FF* recovered to ~75% and ~72% of their initial values.[21] In contrast, P3HT:ICBA devices fabricated with a Ca/Al electrode exhibited no recovery in device efficiency upon thermal annealing in inert atmosphere.[21] For comparison, the degradation profiles for P3HT:PCBM solar cells with a Ca/Ag cathode are shown in Fig. 2(b). The P3HT:PCBM solar cells exhibited a maximum efficiency regeneration of only up to ~15% of the initial value. This recovery in the efficiency of the P3HT:PCBM devices arose primarily from a revival in V_{oc} (up to ~85% of its initial value), whereas J_{sc} only revived up to ~35% of its initial value and no revival in *FF* was observed.[21] As

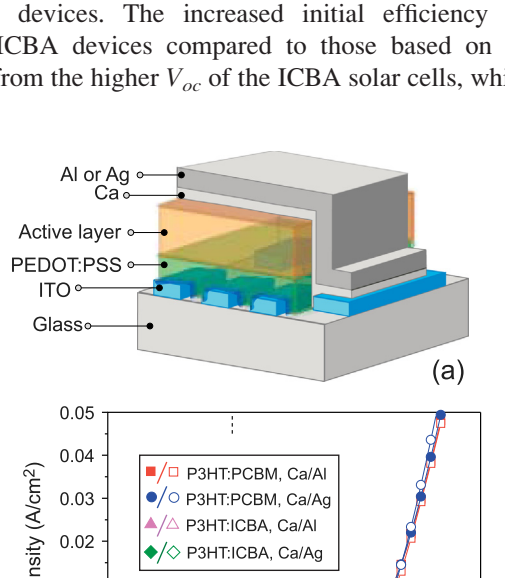

FIG. 1. (a) Schematic of PSCs structures. (b) Dark (solid symbols) and illuminated (open symbols) *J-V* characteristics of fresh solar cells based on the active layers of P3HT:PCBM and P3HT:ICBA with Ca /Al and Ca/Ag cathodes.

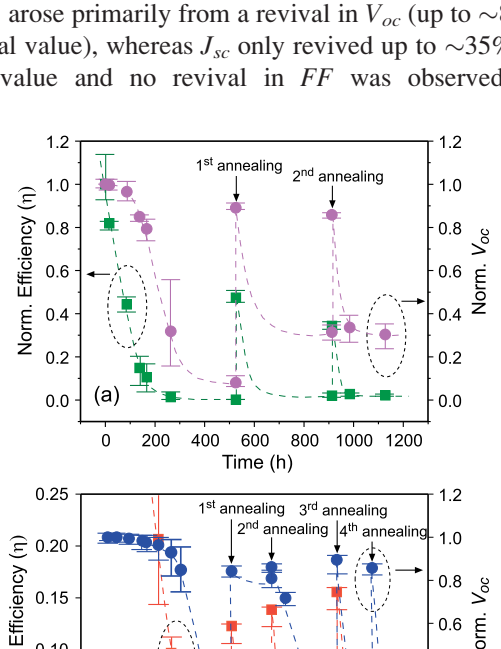

FIG. 2. (a) Degradation profiles of normalized η and V_{oc} for ITO/PEDOT:PSS/P3HT:ICBA/Ca/Ag solar cells with subsequent thermal annealings at different time intervals. (b) Degradation profiles of normalized η and V_{oc} for ITO/PEDOT:PSS/P3HT:PCBM/Ca/Ag solar cells with subsequent thermal annealings at different time intervals.

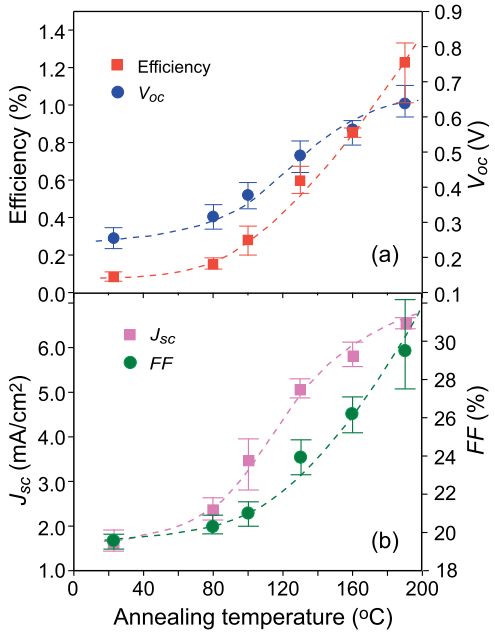

FIG. 3. Effect of annealing temperature on the recovery of (a) efficiency and V_{oc}, (b) J_{sc} and FF of ITO/PEDOT:PSS/P3HT:ICBA/Ca/Ag solar cells.

observed for the P3HT:ICBA devices, P3HT:PCBM devices fabricated with a Ca/Al electrode exhibited no recovery of device performance upon thermal annealing.[21] Previous work on the degradation of P3HT:PCBM devices with Ca/Ag and Ca/Al cathodes has identified that the electrochemical reactions occurring at the interfaces are complex and consist of reversible and irreversible processes.[22] For the Ca/Al electrode, the formation of Al_2O_3 is irreversible and leads to a degradation of device performance. For the Ca/Ag electrode, however the corresponding formation of Ag_2O is a reversible process at ~140 °C under low (~1 ppm) partial pressure of O_2.

In order to establish the origin of the enhanced recovery mechanism in P3HT:ICBA solar cells, the effect of annealing temperature on the regeneration was investigated (Fig. 3). These studies were carried out after the 2nd degradation/annealing cycle on fully degraded devices. Initially, all of the parameters increased systematically with increasing annealing temperature but at high temperatures (>160 °C) both the J_{sc} and V_{oc} tend towards an asymptotic value. Moreover, at these higher temperatures the continued increase in η is primarily driven by a corresponding increase in FF. The close correlation of these recovery profiles as a function of temperature with those observed previously for corresponding P3HT:PCBM devices[22] indicate that the primary cause for the regeneration seen in the P3HT:ICBA devices is also the reversibility of the Ag oxidation process. Further the effect of repeated annealing (140 °C) cycles in an inert atmosphere on the efficiency of pristine P3HT:PCBM and P3HT:ICBA solar cells was also investigated and is shown in Fig. 4(a). Where the P3HT:PCBM solar cells exhibit a rapid reduction in efficiency upon annealing (predominantly because of a correlated reduction in J_{sc}), the P3HT:ICBA solar cells exhibited only a modest reduction (<10%) in efficiency and no deterioration in J_{sc} (Fig. 4(b)).

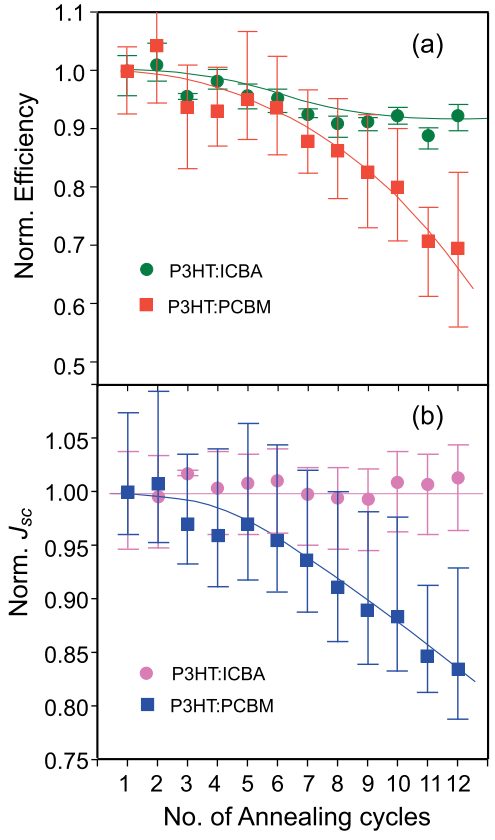

FIG. 4. (a) Effect of subsequent thermal annealings on the efficiency of ITO/PEDOT:PSS/P3HT:ICBA/Ca/Ag and ITO/PEDOT:PSS/P3HT:PCBM/Ca/Ag solar cells. (b) The effect of thermal annealings on J_{sc} of the respective devices.

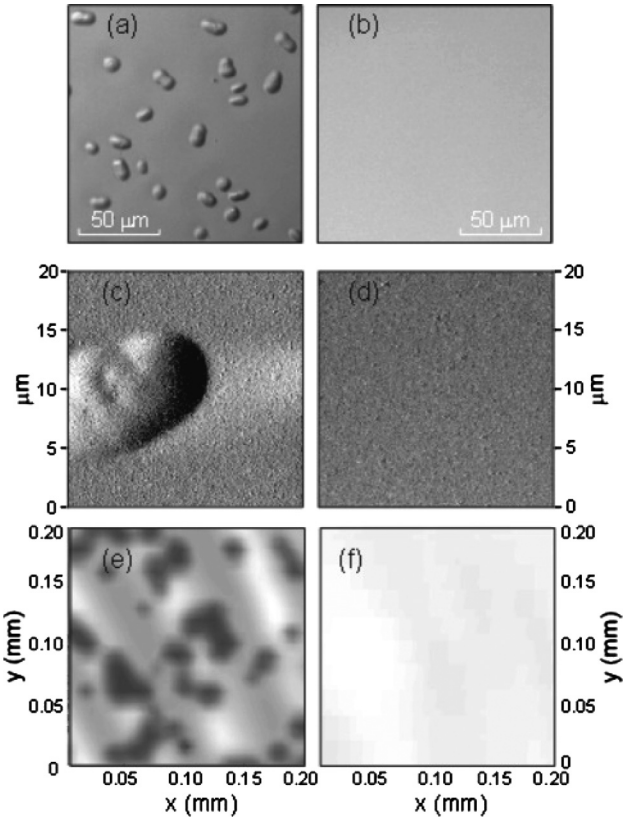

FIG. 5. Optical (above panel), AFM (central panel), and photocurrent mapping (bottom panel) images of ITO/PEDOT:PSS/P3HT:PCBM/Ca/Ag (left panel) and ITO/PEDOT:PSS/P3HT:ICBA/Ca/Ag (right panel) solar cells after 12 subsequent thermal annealings in the glove box.

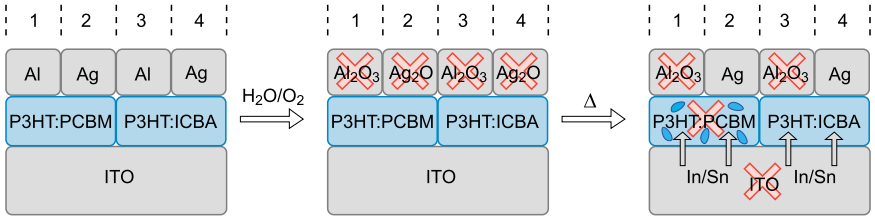

FIG. 6. A schematic of device degradation pathways (indicated by the red crosses) in devices with (1) Al cathode, P3HT:PCBM active layer and ITO anode; (2) Ag cathode, P3HT:PCBM active layer and ITO anode; (3) Al cathode, P3HT:ICBA active layer and ITO anode; and (4) Ag cathode, P3HT:ICBA active layer and ITO anode, upon exposure to water and oxygen and subsequent thermal regeneration.

Previous work has shown that thermal treatment of PSC devices results in irreversible degradation of the anode. For example, for devices with ITO anodes, In and Sn are observed to diffuse into the active layer upon annealing.[22] However, since the electrode structure is the same for both sets of devices the difference in the observed reduction in device performance seen here can only be attributed to changes in the active layer morphology and/or composition.

Previous studies have shown that the spectral and morphological properties of blends of P3HT with PCBM and ICBA are completely different.[23] In particular, upon extended annealing the P3HT:PCBM system undergoes phase segregation to form highly separated component domains, whereas ICBA remains miscible for a wide range of polymer compositions.[23] This different behavior of ICBA can be simply attributed to its structure since ICBA is a bisadduct fullerene possessing two indene side groups, which hinders its crystallization or aggregation. Furthermore, the ICBA material typically consists of a mixture of geometric isomers, again increasing its solubility. The formation of large phase segregated regions is known to lead to device degradation;[1] consistent with the systematic decrease in η and J_{sc} observed in Fig. 4. For the P3HT:ICBA system, however, this phase segregation does not occur and thus there is effectively no loss in J_{sc} after repeated annealing. These conclusions are further supported by the optical, atomic force microscopic (AFM), and photocurrent mapping images of the PSCs after 12 annealing cycles shown in Fig. 5. The optical and AFM images (Figs. 5(a) and 5(c), respectively) clearly show the formation of large ($\sim$10 μm) PCBM aggregates after 12 annealing cycles of the P3HT:PCBM blend films and these aggregates correlate with regions of lower photocurrent generation (dark regions in Fig. 5(e)). By contrast, there is no aggregate formation in the P3HT:ICBA films after 12 annealing cycles (Figs. 5(b) and 5(d)) and there is still uniform photocurrent generation across the film (Fig. 5(f)).

In summary, we can now describe a model for the degradation of these P3HT:Fullerene PSC systems. Device degradation appears to involve three distinct degradation pathways: (1) cathodic oxidation, (2) active layer phase segregation, and (3) anodic diffusion (Fig. 6). Our previous work has shown that cathodic oxidation can be reversed thermally through judicious selection of the cathode materials. In particular, the use of Ag as the cathode material enables cathodic oxidation to be reversed at temperatures that are compatible with the other materials used in the device architecture. In this Letter, we have shown that active layer phase segregation can be mitigated through the use of more miscible organic components. In particular, the use of P3HT:ICBA blends allows PSC devices to be heated to the temperatures required for the regeneration of the Ag cathode without substantially affecting the active layer morphology. Consequently, here we have shown substantial recovery of the performance of fully degraded PSC devices through thermal regeneration, with the devices recovering more than $\sim$50% of their original performance, even after a number of degradation cycles. Since the primary degradation pathway in these devices is now limited to anodic diffusions, work is currently underway to explore alternative anode systems that will mitigate this third degradation pathway and hence fulfill the potential of the demonstrated regeneration process. As such, this work offers the tantalizing prospect of a PSC design that can be fully regenerated through thermal processing.

This project was supported by the Australian Government, through the Australian Renewable Energy Agency (KF). One of the authors (PK) is grateful to the Indian National Science Academy (INSA), New Delhi, for the award of an Early Career Indo-Australia research fellowship to pursue this work in Australia. This work was performed in part at the Materials node of the Australian National Fabrication Facility, which is a company established under the National Collaborative Research Infrastructure Strategy to provide nano and microfabrication facilities for Australia's researchers.

[1]P. Kumar and S. Chand, Prog. Photovolt. **20**, 377 (2012).
[2]J. You, L. Dou, K. Yoshimura, T. Kato, K. Ohya, T. Moriarty, K. Emery, C. C. Chen, J. Gao, G. Li, and Y. Yang, Nat. Commun. **4**, 1446 (2013).
[3]J. You, C. C. Chen, Z. Hong, K. Yoshimura, K. Ohya, R. Xu, S. Ye, J. Gao, G. Li, and Y. Yang, Adv. Mater. **25**, 3973 (2013).
[4]Z. He, C. Zhong, S. Su, M. Xu, H. Wu, and Y. Cao, Nat. Photonics **6**, 591 (2012).
[5]R. F. Service, Science **332**, 293 (2011).
[6]M. A. Green, K. Emery, Y. Hishikawa, W. Warta, and E. D. Dunlop, Prog. Photovolt. **21**, 1 (2013).
[7]O. Adebanjo, P. P. Maharjan, P. Adhikary, M. Wang, S. Yang, and Q. Qiao, Energy Environ. Sci. **6**, 3150 (2013).
[8]M. Jorgensen, K. Norrman, S. A. Gevorgyan, T. Tromholt, B. Andreasen, and F. C. Krebs, Adv. Mater. **24**, 580 (2012).
[9]T. D. Nielsen, C. Cruickshank, S. Foged, J. Thorsen, and F. C. Krebs, Sol. Energy Mater. Sol. Cells **94**, 1553 (2010).
[10]P. Kumar, A. Sharma, and D. P. Singh, Prog. Photovolt. **21**, 950 (2013).
[11]F. C. Krebs, *Stability and Degradation of Organic and Polymer Solar Cells* (John Wiley & Sons, Ltd., 2012).
[12]M. Jorgenson, K. Norrman, and F. C. Krebs, Sol. Energy Mater. Sol. Cells **92**, 686 (2008).
[13]K. Norrman, M. V. Madsen, S. A. Gevorgyan, and F. C. Krebs, J. Am. Chem. Soc. **132**, 16883 (2010).
[14]H. B. Yang, Q. L. Song, C. Gong, and C. M. Li, Sol. Energy Mater. Sol. Cells **94**, 846 (2010).
[15]K. Kawanoa, R. Pacios, D. Poplavskyy, J. Nelson, D. D. C. Bradley, and J. R. Durrant, Sol. Energy Mater. Sol. Cells **90**, 3520 (2006).

[16]J. A. Hauch, P. Schilinsky, S. A. Choulis, R. Childers, M. Biele, and C. J. Brabec, Sol. Energy Mater. Sol. Cells **92**, 727 (2008).
[17]M. P. Nikiforov, J. Strzalka, and S. B. Darling, Sol. Energy Mater. Sol Cells **110**, 36 (2013).
[18]Y. Sun, C. J. Takacs, S. R. Cowan, J. H. Seo, X. Gong, A. Roy, and A. J. Heeger, Adv. Mater. **23**, 2226 (2011).
[19]S. K. Hau, H. L. Yip, and A. K. Y. Jen, Polym. Rev. **50**, 474 (2010).
[20]F. Cheng, G. Fang, X. Fan, H. Huang, Q. Zheng, P. Qin, H. Lei, and Y. Li, Sol. Energy Mater. Sol. Cells **110**, 63 (2013).
[21]See supplementary material at http://dx.doi.org/10.1063/1.4878408 for degradation profiles of normalized J_{sc} and *FF* for ITO/PEDOT:PSS/P3HT:ICBA/Ca/Ag and for ITO/PEDOT:PSS/P3HT:PCBM/Ca/Ag solar cells, and normalized efficiency for ITO/PEDOT:PSS/P3HT:ICBA/Ca/Al and ITO/PEDOT:PSS/P3HT:PCBM/Ca/Al solar cells.
[22]P. Kumar, C. Bilen, K. Feron, N. C. Nicolaidis, B. B. Gong, X. Zhou, W. J. Belcher, and P. C. Dastoor, ACS Appl. Mater. Interfaces **6**, 5281 (2014).
[23]Y. H. Lin, Y. T. Tsai, C. C. Wu, C. H. Tsai, C. H. Chiang, H. F. Hsu, J. J. Lee, and C. Y. Cheng, Org. Electron. **13**, 2333 (2012).